

GAS ABSORPTION WITH CHEMICAL REACTION

by

CHUNG-KONG HWU

B. S., National Taiwan University, China, 1951

A THESIS

submitted in partial fulfillment of the

requirements for the degree

MASTER OF SCIENCE

Department of Chemical Engineering

KANSAS STATE COLLEGE
OF AGRICULTURE AND APPLIED SCIENCE

1954

LD
2668
T4
1954

H9
C.2
Documents

TABLE OF CONTENTS

INTRODUCTION AND REVIEW OF LITERATURE..... 1
PURPOSE AND SCOPE OF STUDY.....13
CONSTRUCTION OF EQUIPMENT.....15
OPERATION PROCEDURE.....30
CHEMICAL ANALYSIS.....31
SUMMARY OF DATA.....33
RESULTS AND DISCUSSION.....34
CONCLUSION.....48
ACKNOWLEDGMENTS.....50
BIBLIOGRAPHY.....51
APPENDIX.....53
 Calibration of Flowmeters.....54
 Evaluation of Chemical Analysis.....57
 Sample Calculation.....60
 Calculation of Surface Velocity of Falling Film.....68
 Principal Constants of the Disc Column.....71
 Nomenclature.....71

INTRODUCTION AND REVIEW OF LITERATURE

In most of the industrial gas absorption processes, it frequently involves a chemical reaction between the solute gas and some component within the liquid phase. The mechanism of such mass transfer process is one of physical solution followed by a chemical reaction which may take place in several ways:

Case I. Reaction taking place at the surface of liquid: rate of absorption is controlled by the gas film and this process is similar to that of the physical absorption.

Case II. Reaction taking place in a narrow zone within the liquid film: this occurs when the rate of reaction is rapid compared with the rate of diffusion of reactants and products. In this case, the rate of absorption is controlled by diffusion in the liquid.

Case III. Reaction taking place during the diffusion of the dissolved gas through the liquid film: rate of absorption is controlled by both the reaction and diffusion rate.

Case IV. Reaction taking place in the main body of the liquid: there are again two possible ways for this mechanism: (a) the reaction proceeds at a moderately slow rate and the concentration of the dissolved gas in the liquid film has such a value that the rate of removal of the solute gas by reaction is balanced by the rate of diffusion of solute gas to the liquid; (b) the reaction proceeds very slowly and the concentration of the dissolved gas in the liquid may be saturated relative to the gas phase. The

rate of absorption is entirely controlled by the reaction velocity.

The gas absorption mechanisms based on the two-film concept are illustrated in a series of idealized sketches in Fig. 1. In purely physical absorption where there is no chemical reaction involved, the solute gas is the only diffusing molecular species. In such case, it is convenient to represent the resistance to mass transfer by some "effective" thickness of the stagnant films on either side of the interface even though the actual existence of such stagnant films under packed column conditions is questionable and will be discussed later. When there are chemical reactions involved, in addition to the net movement of solute gas across the interfacial boundary, the reactant is moving into the "reaction zone" where the reactions take place, and the product and unreacted solute are moving out of the "reaction zone." The depth of the reaction zone varies from zero in Case I to infinity in Case IV. There is no straight-forward correlation between the reaction zone and the assumed stagnant films of finite resistance but negligible holding capacity. Furthermore, unless the reaction is instantaneous and irreversible, the concentration gradient across the films or throughout the zone varies with time. This means that the depth of the reaction zone is a function of the history of the film. Therefore, the extension of the two-film concept to cover the simultaneous chemical reaction and physical absorption is not as simple as it may appear. Consequently, the diagrams in Fig. 1 only represent the probable presence of solute gas, reactant and product at various distance from the interface at some finite time

No chemical reaction; both gas and liquid side resistance are appreciable.

Case I. Instantaneous chemical reaction taking place at the liquid surface.

Case II. Fast reaction taking place in a narrow zone in the liquid film.

Case III. Reaction taking place at moderate rate during the diffusion through the film.

Case IV. Slow reaction taking place in the bulk of liquid

(a) Rate of the diffusion of the solute gas into the film equals the rate of removal from the film by chemical reaction.

(b) Liquid film is saturated with the solute gas.

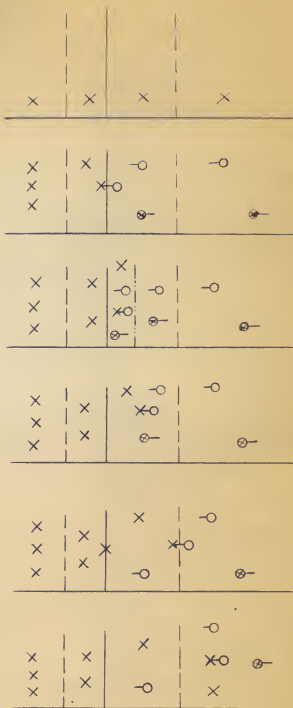


Fig. 1. Gas absorption mechanisms based on the two-film concept.

after the gas-liquid contact has been made.

Theoretical treatment has been made for some particular cases of these reaction mechanisms by various authors. A brief review of the theories and previous work on the gas absorption with chemical reaction is presented as the background of the current investigation.

Based on Hatta's (7) equation which was developed from his experiment of batch absorption of CO_2 in KOH solution, Sherwood and Pigford (20) derived an equation for rapid second-order, irreversible reaction taking place in a narrow zone of the liquid phase. (Case II)

$$N_A = \frac{(p/H) + (D_B/D_A)q}{(x_L/D_A) + (1/k_G)} \quad (1)$$

where N_A = rate of mass transfer per unit area

p = partial pressure of solute gas

H = Henry's law constant, defined by $p = HC$

$D_{B,A}$ = diffusivity of the dissolved gas molecule and liquid reactant, respectively

x_L = fictitious liquid-film thickness

k_G = gas-phase coefficient

q = concentration of liquid absorbent

By eliminating the gas phase resistance, the following equation results

$$N_A = \frac{D_A}{x_L} \left[C_{A_i} + \frac{D_B q}{D_A} \right] \quad (2)$$

where C_{A_i} = concentration of the dissolved gas molecule at the interface at equilibrium with the solute partial pressure over the interface.

The liquid film coefficient is defined on the assumption that there is no free gas in the main body of the liquid.

$$k_L = \frac{D_A}{x_L} \left[1 + \frac{D_0}{D_A} \frac{q}{C_{A1}} \right] \quad (3)$$

The term $\frac{D_A}{x_L}$ in the equation is the liquid film coefficient for physical solution under the same operation condition.

Hata (7) presented another equation for slow first-order reaction by assuming the concentration of the free dissolved gas was zero or negligible. (Case III)

$$N_A = \frac{D_A (C_{A1} - C_L)}{x_L} \frac{\lambda_L \sqrt{\frac{k_I}{D_A}}}{\tanh \lambda_L \sqrt{\frac{k_I}{D_A}}} \quad (4)$$

where k_I = first-order reaction rate constant

C_L = bulk liquid concentration

Van Krevelen and Hoftizzer (30) considered that the gas absorption process with a slow first-order reaction is rare. They derived an equation for k_L for packed towers with the assumptions made that the reaction is of slow second order and that the concentration of the dissolved solute gas in the liquid film is nearly constant. (Case III)

$$\frac{k_L \left(\frac{\mu^2}{g P^2} \right)^{1/2}}{D} = 0.015 \left(\frac{L}{a \mu} \right)^{2/3} \left(\frac{\mu}{P D} \right)^{1/2} \frac{\chi}{\tanh \chi} \quad (5)$$

$$a = a_d - a_d e^{-0.40(L/P)}$$

$$\chi = \left(\frac{\mu^2}{g P^2} \right)^{1/2} \left(\frac{k_{II} C_A}{D} \right)^{1/2}$$

and C_A = concentration of dissolved solute

μ = viscosity of the liquid

ρ = density of the liquid

L = liquid rate, mass/time, area

k_{II} = second-order reaction rate constant

a = effective area, ft.²/ft.³

D = diffusivity of solute gas in liquid

When $k_{II} = 0$, this equation reduces to

$$\frac{k_L \left(\frac{\mu^2}{\rho^2 g} \right)^{1/3}}{D} = 0.015 \left(\frac{L}{a\mu} \right)^{2/3} \left(\frac{\mu}{\rho D} \right)^{1/6} \quad (6)$$

This is identical with that for physical absorption. When $k_{II} C_A$ is relatively large, equation (5) can also be simplified to

$$\frac{k_L \left(\frac{\mu^2}{g \rho^2} \right)^{1/3}}{D} = 0.015 \left(\frac{L}{a\mu} \right)^{2/3} \left(\frac{\mu}{\rho D} \right)^{1/3} \left(\frac{\mu^2}{g \rho^2} \right)^{1/3} \left(\frac{k_{II} C_A}{D} \right)^{1/2} \quad (7)$$

They used the data of Tepe and Dodge (25), Payne and Dodge (14), Furnas and Bellinger (3) as well as their own data on absorption of CO₂ in alkaline solution and in ammonical solution. The k_{II} was calculated and an average value was found to be 0.019 + 23%.

As shown in these theoretical developments, the film coefficient for a chemical absorption process may be expressed as some function of a number of variables as defined previously:

$$k_L = f(Re_L, Sc_L, k, C, C_1, D_B, D_A). \quad (8)$$

In reviewing the previous experimental determinations, the rate of transfer has been found to be dependent on some of the factors in equation (8). Some of the data gave support to the theories qualitatively. Jenny (10) used a stirred batch absorber to study the

absorption of ethyl acetate, methyl formate and CO_2 in NaOH . He found that the rate of absorption of ethyl acetate by NaOH was controlled by the gas phase resistance, but the time required for reaction to complete was appreciable. The absorption of methyl formate in NaOH was, however, affected by concentration of the NaOH . The transfer coefficient, he found, was proportional to the normality of NaOH and inversely proportional to the solute gas partial pressure. In his experiment on the absorption of CO_2 in NaOH using the same apparatus, he found that the transfer coefficient was constant at a value of $0.028 \text{ lb. mole/hr. ft.}^2 \text{ atm.}$ when the concentration of NaOH was above 1 N. This should be the gas film coefficient, according to Hatta's assumption of a rapid second-order reaction in a narrow zone of the liquid film. Hatta pointed out that, if the liquid concentration is over a certain value, the liquid phase resistance is unimportant, and the rate of transfer is controlled by the gas-phase resistance. However, k_G turned out to be $0.187 \text{ lb. mole/hr. ft.}^2 \text{ atm.}$ in a separate experiment on absorption of ammonia in water, which would predict a considerably higher rate than what was observed. Jenny explained, in this case, that the absorption was limited by the rate at which CO_2 was able to combine chemically with OH ions.

Pozin (17) used a wetted wall column for studying the systems of CO_2 in NaOH , KOH or Na_2CO_3 as well as Cl_2 in NaOH . His data showed that the rate of transfer was proportional to the ratio of the normality of liquid and the solute gas partial pressure, which was in agreement with Hatta's assumption of rapid second-order reaction within a narrow zone in the liquid film.

Tepe and Dodge (25) carried out an extensive study on the absorption of CO_2 in KOH or NaOH using a 6-inch packed column with 0.5 in Raschig rings. Their data indicated that the rate of transfer was not affected by the rate of gas flow, but it was affected by the liquid rate. The transfer coefficient increased with increasing alkaline normality up to 2 N. Above this value, the transfer coefficient decreased slightly because of the increasing value of the liquid viscosity. In all concentrations, the absorption rate increased with temperature. They also found in their experiment that the reaction of CO_2 and NaOH was a slow pseudo first-order reaction occurring throughout the entire liquid film simultaneously with diffusion (Case III). Spector and Dodge (23), with the same system, found that the transfer coefficient was 20-30 per cent greater when absorbing CO_2 in KOH instead of NaOH. They found that the gas film coefficient was significant but not predominate.

Turkhan (29) measured rates of absorption of CO_2 from air in sodium hydroxide in a batch process. He found that the rate of transfer was not affected by the normality of the alkali when its concentration exceeded a critical value. This result confirms Hatta's assumption, as explained previously (p. 7).

Theories based on the unsteady-state-diffusion concept proposed by Higbie (8) have been developed for slow first-order reaction and for rapid second-order reaction taking place in the liquid film. These have been reported by Sherwood and Pigford (20).

Danckwerts (2) suggested, without experimental proof, a new

concept of the gas absorption mechanism. The assumption of a stagnant film of liquid at the interface was abandoned. Instead it was supposed that the surface was continually being replaced with fresh liquid, and on this basis equations for the absorption rates have been derived for the following cases: (a) Surface constantly saturated, no chemical reaction; (b) Gas-film resistance, no chemical reaction; (c) Surface resistance, no chemical reaction; (d) Solute destroyed by first-order reaction with solvents; (e) Instantaneous reaction between dissolved gas and reagent in solution; (f) Second-order reaction between dissolved gas and reagent in solution.

Equations were developed to express the rate of mass transfer as a function of a number of physical constants:

For physical absorption,

$$N_A = F (s, D, C, k_G, k_S) \quad (9)$$

where s = the rate of renewal of the liquid surface

k_S = surface transfer coefficient

and for chemical absorption,

$$N_A = F' (s, D, C, k_G, k) \quad (10)$$

where k = reaction rate constant

However, the verification of this new mechanism seems awkward in the present state of knowledge because of the lack of the necessary information such as the turbulence condition and the surface transfer coefficient.

From the review of the present state of development, two conclusions can be drawn: (1) quantitative formulations have been

worked out only for a few idealized chemical reaction mechanisms; and (2) the experimental data have been established for only a few simple systems, and even these simple systems cannot all be correlated by the theoretical formulation.

For design purpose, data must be obtained from experimental determination of the transfer coefficients by means of suitable apparatus. Among all the existing apparatus for industrial absorption process as well as for research, the packed column is one of the most common and most important units, but the behavior of which is relatively complex, since it involves two fluids flowing over the packing in direct contact. The behavior of each stream will have some effect on the other. Furthermore, based on the two-film concept, the transfer coefficient is a function of the film thickness. Much of the factors, such as viscosity, density, flow rate, etc., that affect the films will in turn affect the coefficients. Also, the wetting condition in the column of this type is scarcely known. The actual wetted area of the packing is uncertain. The experimental work for final design must be carried out through a semi-work scale column packed with the same packing and operating at the same condition as that being designed for, and the cost for constructing and operating the column is high.

Wetted wall column has been widely employed in the laboratory to study the gas absorption problems. The advantage of this column is that the wetted area is known and the turbulence condition in the gas stream are reproducible. With this advantage, the wetted wall column can be used as a tool for testing the various

correlation methods and to establish the mechanism of gas absorption for the systems studied. Extensive work has been done with the wetted wall column for systems in which the rate of transfer is controlled by the gas phase resistance, such as Gilliland and Sherwood's (4) measurement of the rate of evaporation of several kinds of liquid in air. Their result could be correlated by the simple empirical equation:

$$\frac{k_G P_{IM}}{G_M} = 0.023 (Re)^{-0.17} (Sc)^{-0.56} \quad (11)$$

where k_G = gas-film coefficient

P_{IM} = mean partial pressure of inert gas

Re = Reynold number, defined as $\frac{vd\rho}{\mu}$, v , relative velocity to the liquid surface; d , diameter to the gas flow; ρ , density of gas mixture; μ , viscosity of gas mixture.

Sc = Schmidt group, defined as $\frac{\mu}{\rho D}$,
 d , diffusivity of solute gas in gas phase.

G_M = mass rate of gas, mass/time, area

which is similar to the correlation of heat transfer by convection in a round pipe. This also gave support to the film concept of mass transfer mechanism. However, use of wetted wall column data to correlate the liquid film transfer coefficient has not been so successful. Grimley (5), in his extensive study on absorption of carbon dioxide, found that the resistance to transfer was less than that would be expected from the theory. He explained that this discrepancy was caused by the ripple formation at the liquid surface. Also the transfer coefficient is dependent on the length of the column.

A new type of research column was designed by Stephens and Morris (24). It consists of a single strand of small discs (threaded edgewise) suspended vertically at the center of a small pyrex column (about 1 inch in diameter). The liquid flows downward over the discs. The surface of the liquid is interrupted while flowing from disc to disc. Thus, the flow condition is similar to that of the packed column. (Particularly the Stedman type packing.) The surface of the absorption element is always wetted and the contact area of which can be estimated. Therefore, it possesses the advantage of both packed and wetted wall column. The construction and operating cost is low because of the small size. In their experiment on absorption of CO_2 or NH_3 in H_2O , Stephens and Morris found that the transfer coefficient did not vary by varying the number of discs. The result obtained was similar to those by Sherwood and Holloway (21) and by Gilliland and Sherwood (4). These indicated the suitability of this type of column for research as well as for design purpose. This column is particularly suitable for the determination of liquid film coefficient, especially for systems involving chemical reaction in the liquid layer.

Stephens and Morris (24) used the disc column for the system of Cl_2 in air and the aqueous solution of ferrous chloride and ferric chloride. Their result indicated that the effect of the ferrous chloride concentration C_B could not be separated from the effect of the concentration of dissolved chlorine at the interface. The fractional increase in liquid film coefficient due to chemical reaction was found to be

$$\frac{k_L}{k'_L} - 1 = 0.75 \left(\frac{C_B}{C_1} \right)^{0.83} \quad (12)$$

within a range of C_B/C_1 from 0 to 1,200,

where k_L = liquid-film coefficient for chemical absorption

k'_L = liquid-film coefficient for physical absorption alone

C_B = bulk concentration of liquid

C_1 = dissolved solute gas concentration at the interface

Several months after the construction of the disc column for the present investigation had begun, Roper (18) in England reported his study on the absorption of chlorine from air by solution of 2-ethyl hexene-1 in carbon tetrachloride in presence of iodine as catalyst. He used the same method as employed by Stephens and Morris. The fractional increase in liquid film coefficient due to chemical reaction was found to be

$$\frac{k_L}{k'_L} - 1 = 39.2 \frac{(C_0 + 0.00005)}{C_1} 0.5 \quad (13)$$

where C_0 is the concentration of iodine content.

PURPOSE AND SCOPE OF STUDY

The objective of this research was to design, construct, and calibrate a disc column as a versatile piece of research tool and to perfect the operational and analytical procedures as a guide to subsequent studies on various new chemical systems.

The absorption of CO_2 in water was studied with this column to determine the liquid phase transfer coefficient because CO_2 is

relatively insoluble in water and the gas phase resistance is not appreciable (21). The overall transfer coefficient based on the liquid concentration obtained was considered to be equal to the liquid phase transfer coefficient. Also the absorption of dilute NH_3 in air by water was studied to determine the gas phase transfer coefficient of this column. The total resistance to transfer for this system had been considered to be on the gas phase side previously until Whiteman and David (31) pointed out that there was an appreciable resistance on the liquid phase. This was confirmed by Sherwood and Holloway (22). Therefore, overall resistance based on the partial pressure of the solute gas is the sum of the resistance contributed by the gas film and the liquid film. The gas phase transfer coefficient could be obtained by deduction of the liquid phase transfer coefficient which was determined by the CO_2 runs from the overall coefficient. Empirical equations similar to those obtained by Sherwood and Holloway (21) and Gilliland and Sherwood (4) relating the transfer coefficients with the possible variables were developed for this column for use in systems other than those employed in the present experiment.

For each new column, because of the particular dimensions and the nature of the surface of the discs, it may have a set of transfer coefficients numerically different from another column. Thus, the "calibration" procedure was necessary. The studies on CO_2 and NH_3 were designed to accomplish two things: (1) to ascertain that the characteristics of the disc column do resemble those of the conventional packed column; that is, to see if the observed transfer coefficient can be correlated by the equations similar to those

proposed for packed column; and (2) to establish the characteristic gas-film coefficient of the column. Once this is done, it is proposed that for any other new system under study the liquid-film coefficient can be estimated by subtracting the gas-film coefficient from the observed overall transfer coefficient. Note that the coefficient thus estimated would not apply to the final column design directly. For that purpose, the quantitative correlation between the disc column performance and other packings must be established first. Although such correlation has been deemed promising (24), the primary concern of this research was to provide a laboratory tool for evaluating the effect of concentration and flow variables upon the liquid-film coefficient, thereby throwing some light on the combined mechanism of diffusion and chemical reaction in the liquid phase.

CONSTRUCTION OF EQUIPMENT

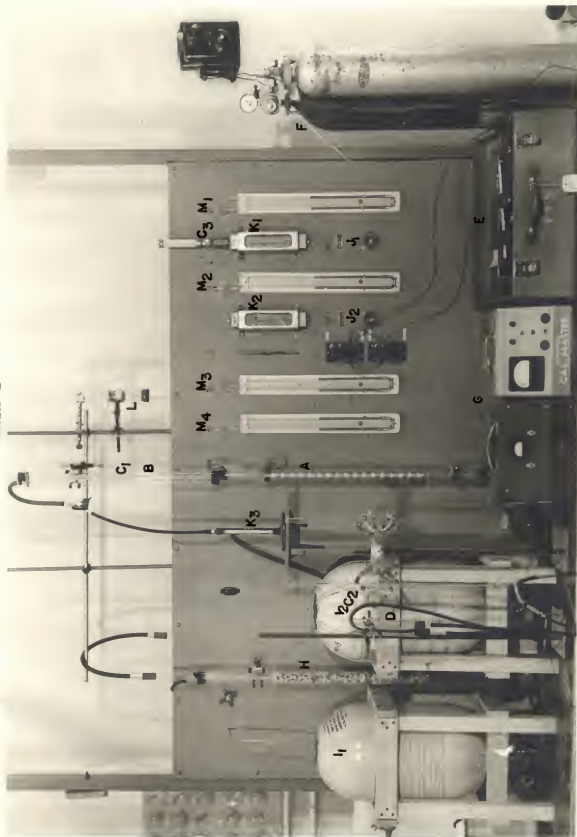
The equipment used is shown in Plates I and II. The general arrangement of the disc column is shown in Plates III and IV, and the principal dimensions are given in the Appendix (p. 71). The absorption column was made of Pyrex with an inside diameter of $1 \frac{1}{8}$ inches, a wall thickness of $\frac{1}{16}$ inch, and a height of 34 inches. Two side arms with a bore of $\frac{1}{2}$ inch were located near the two ends. They were bended in right angle so that it would be possible for the addition of a water jacket for further absorption studies at controlled temperature levels.

Thirty-five ceramic discs with unglazed surfaces were used in

EXPLANATION OF PLATE I

- A. Disc column
- B. Liquid feed cylinder
- C₁, C₂. Thermocouples for measuring liquid temperature
- C₃. Thermometer for measuring gas temperature
- D. Liquid sampler
- E. Potentiometer
- F. Gas cylinders
- G. Thermoconductivity cell with a helper unit
- H. Packed column for scrubbing residue solute gas from exit.
- I₁, I₂. Stainless steel liquid storage tank
- J₁, J₂. 1/4 inch stainless steel controlling needle valve
- K₁, K₂. Rotameters for inert and solute gas respectively
- K₃. Flowrator for liquid.
- L. Wet-bulb thermocouples
- M₁, M₂. Manometers for measuring inert and solute gas pressure respectively
- M₃, M₄. Manometers for measuring column pressures at inlet and at outlet respectively

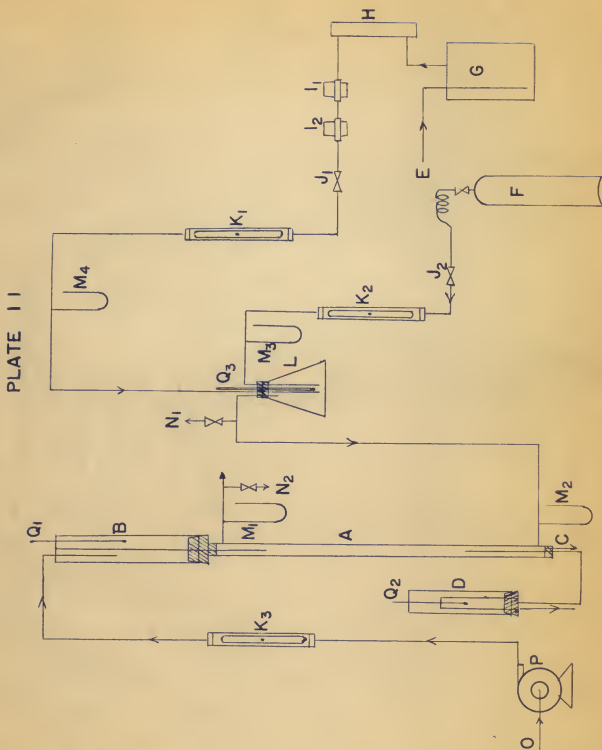
PLATE I



EXPLANATION OF PLATE II

Schematic Diagram of Equipment Layout

- A. Disc column
- B. Liquid feed cylinder
- C. Drain for liquid lost by splash
- D. Liquid sampler
- E. Air inlet
- F. Solute gas cylinder
- G. Air surge tank
- H. Air filter
- I₁, I₂. Pressure reducers
- J₁, J₂. Needle valves
- K₁, K₂, K₃. Rotameters
- L. Gas mixer
- M₁, M₂, M₃, M₄. Manometers
- N₁, N₂. Gas sampling points
- O. Liquid inlet
- P. Centrifugal pump
- Q₁, Q₂, Q₃. Thermometers

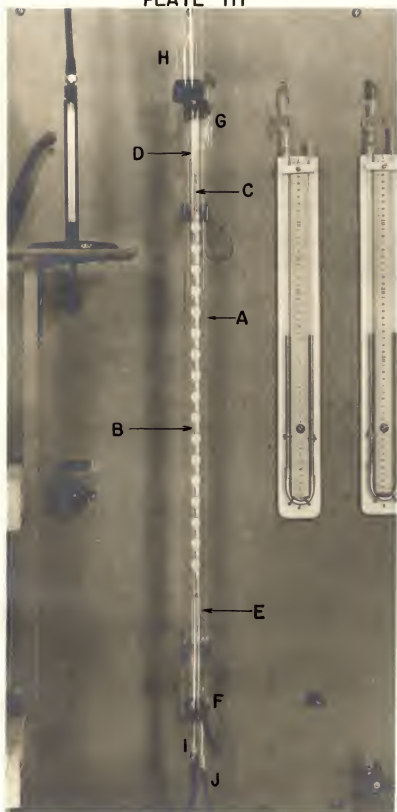


EXPLANATION OF PLATE III

Close-up View of Disc Column

- A. Pyrex tube
- B. Ceramic discs
- C. Supporting Fiberglas cord
- D. Liquid feed jet
- E. Long stem funnel
- F. Gas inlet
- G. Gas outlet
- H. Liquid feed cylinder
- I. Effluent to liquid sampler
- J. Drain for liquid lost by splash

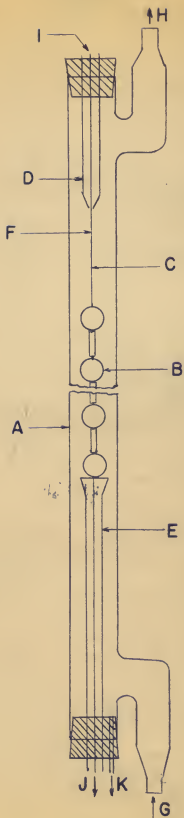
PLATE III



EXPLANATION OF PLATE IV
Arrangement of Disc Column

- A. Pyrex tube, 1 1/8 in. i. d., 34 in. long
- B. Ceramic disc, 1.5 cm. in diameter and 0.48 cm. in thickness
- C. Distance between jet and first disc to be 4-5 cm.
- D. Liquid feed jet
- E. Long stem funnel
- F. Supporting Fiberglas cord, held externally
- G. Gas inlet
- H. Gas outlet
- I. Liquid inlet
- J. Effluent to liquid sampler
- K. Drain for liquid lost by splash

PLATE IV



this study. The discs were threaded edgewise upon a 1.5 mm. Fiberglass cord, and successive discs were maintained at right angles by means of Duco cement. The series of discs were mounted vertically and centrally in the column and maintained under tension by a spring attached on the top of the feed cylinder.

Liquid was pumped from two stainless steel storage tanks by a one-half horsepower centrifugal pump through a Fisher and Porter C-Clamp Flowrator, then into a Pyrex feed cylinder with 45 mm. inside diameter located directly above the column. The Flowrator was calibrated by collecting and weighing the discharge. Liquid then flowed by gravity through the "feed jet" into the top of the disc column. The jet consisted of a straight piece of Pyrex tubing with a bore of 10 mm. and an opening of 4 mm. at one end. Extruding from the base of the feed cylinder, the restricted end was placed about 4 to 5 cm. above the uppermost disc. After flowing downward on the surface of the discs, the liquid was withdrawn through a long stem funnel into the liquid sampler at adjustable level. The height of the feed cylinder and the opening of the feed jet were dictated by the flow rate and the operating gas pressure inside the column.

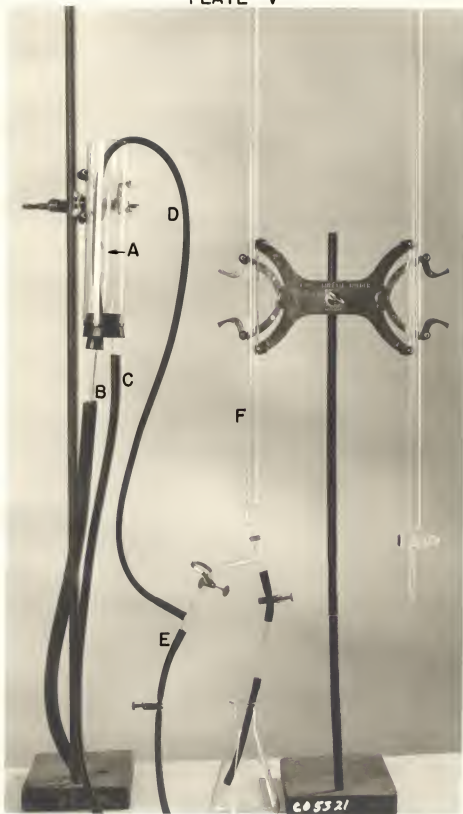
The sampler, as shown in Plate V, consisted of an overflow arrangement with two Pyrex tubes placed concentrically. The diameters of the outer tube and the inner tubes were so chosen that the inner tube was small enough to reduce the chance of longitudinal mixing of the effluent but large enough for the provisions of temperature measurement as well as sampling. The liquid sample was siphoned off with a piece of rubber tube which was connected

EXPLANATION OF PLATE V

Arrangement of Liquid Sampler

- A. Inner, overflow tube
- B. Liquid from column
- C. Overflow to drain
- D. Siphon tube
- E. Drainage
- F. Buret for measuring sample volume

PLATE V



through a glass tee to a buret for measuring the volume of sample. The liquid was kept flowing continuously through the sampling system during operation.

During the absorption runs of CO_2 in H_2O , CO_2 from the cylinder was passed into the column directly through a Brooks rotameter. The method of calibration of the rotameters is given in the Appendix (p. 54). Provision was made for the measurement of wet-bulb temperature of the exit CO_2 . Chromel-alumel thermocouples were used in temperature measurement. The thermocouple serving as the wet-bulb thermometer was wrapped, at the junction, with cotton yarn which was kept wet constantly. The pair of dry-bulb and wet-bulb thermocouple wires were supported with 8-inch sections of Pyrex tubing, and the joints were placed in direct passage of the exit gas from the column. To increase the linear velocity of the gas stream, the exit gas was first forced through a 3 mm. jet (Plate VI).

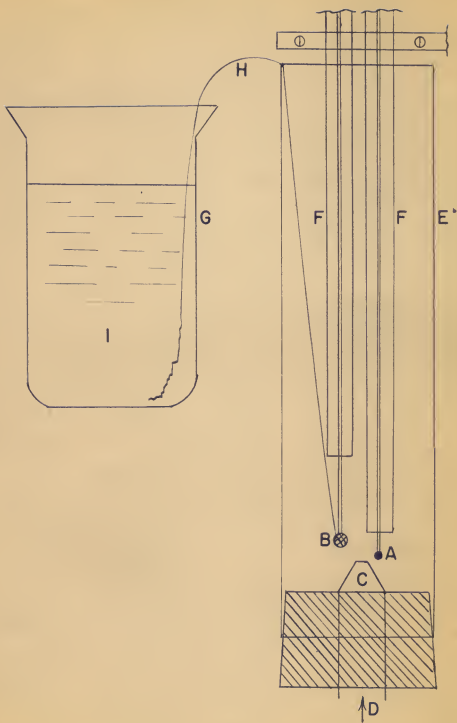
Mixtures of air and NH_3 were used in the absorption of NH_3 in water to investigate the gas phase transfer coefficient by this column. The concentration of NH_3 in the gas mixture was about 2 to 5 per cent by volume. High pressure air from the power plant was passed through a surge tank then a filter containing silica gel and glass wool in order to remove or reduce the moisture, oil, and other entrainment. The flow was controlled by two pressure reducers and a 1/4-inch needle valve and measured by a Fisher and Porter type Flowrator. NH_3 from cylinder was measured and controlled by Flowrator and a needle valve respectively. The two streams of gases were brought together and well-mixed in a 2000 cc.

EXPLANATION OF PLATE VI

Arrangement of Wet-bulb Thermometers

- A. Dry-bulb thermocouple
- B. Wet-bulb thermocouple wrapped with cotton yarn
- C. Jet
- D. Exit gas from column
- E. Pyrex tube
- F. Supporting glass tubing
- G, I. Beaker containing distilled water
- H. Cotton yarn for supplying water to wet-bulb thermocouple

PLATE VI



Erlenmeyer flask. The gas mixture then entered at the base of the disc column and released to atmosphere. Gas pressures were measured by means of manometers located downstream from the Flowrators. Column pressures were measured by manometers at the gas inlet and exit of the column. Either water saturated with solute gas or mercury was used for the medium in the manometers according to the operating pressure range.

The temperature of the gas mixture was measured with a mercury bulb thermometer inserted in the mixing flask, and that of the liquid was measured by two chromel-alumel thermocouples dipped in the feed cylinder and in the sampler.

A Pyrex tube 3 feet long with 45 mm. inside diameter and packed with $\frac{1}{2}$ -inch Berl Saddle packing was provided for scrubbing the NH_3 in exit gas. An aspirator was used to create vacuum in this small packed column in order to reduce the inlet gas pressure at the disc column. However, in the actual NH_3 runs, the exit NH_3 concentration was found to be so low that the scrubbing process was not considered necessary.

OPERATION PROCEDURE

In starting up, the sampler was moved up and down to flush the air bubbles out of the effluent passage. Then, placing the sampler at the lowest possible level, water was pumped into the feed cylinder at a high rate (about 45 lbs./hr.) in order to wet the surface of the discs entirely. Next, gas was turned on slowly. A sudden increase in the gas rate would cause the gas to rush out of

the column through the feed jet before a liquid head was built up in the liquid feed cylinder to balance the gas pressure inside the column. Meanwhile the sampler was raised to a position to bring the liquid level up to the neck of the long stem funnel inside the column in order to avoid any additional absorption surface formed by a liquid film on the inside of the funnel stem. In the runs of absorption of ammonia in water, inert gas was turned on first and then the solute gas.

The flowmeter readings were checked from time to time to insure the rates of gas and liquid were constant. Steady state conditions would normally be reached in one hour after starting the operation. Samples were then taken every ten minutes. The operation was not completed until three successive analyses of the sample showed consistency. Gas and liquid rates were regulated to another range and the next run was continued. Temperatures, pressures, and flowrates were duly recorded during the run.

CHEMICAL ANALYSIS

Ammonia in H_2O

The analysis of ammonia in water was accomplished by running the liquid sample into a 250 cc. Erlenmeyer flask containing a measured amount of standard H_2SO_4 (19). After a few minutes with occasional shaking, the excess H_2SO_4 was back titrated with standard NaOH to a methyl orange end-point. One cc. of 0.1N H_2SO_4 consumed is equivalent to 0.0017 gm. of NH_3 .

Ammonia in Air

A Gow-Mac thermoconductivity cell (Gas-Master Unit) was originally attempted for the analysis of N_2-NH_3 and air- NH_3 gas mixtures. However, since the thermal conductivity of these component gases are so close together ($k_{NH_3} = 0.0095$, at $-76^\circ F.$, $k_{N_2} = 0.0095$ at $-148^\circ F.$, $k_{air} = 0.0095$ at $-148^\circ F.$) and the composition of NH_3 in gas mixture was so low that this means of analysis was not successful. Therefore, no attempt was made to establish the material balance across the column. All the calculations were based on the liquid analysis.

Water in CO_2 Gas

During the test runs, it was observed that the water evaporated into the stream of CO_2 was appreciable. The determination of moisture content in the exit CO_2 was made by measuring the wet-bulb temperature depression of the exit CO_2 with a pair of wet and dry-bulb thermocouples as described previously. The amount of moisture in gas was interpolated from a humidity chart (9). Partial pressure of CO_2 was obtained by deduction of the partial pressure of water from the total pressure of the exit gas stream.

CO_2 in Water

Three methods of analysis of CO_2 in H_2O were investigated and compared during the test runs. They were: (1) method proposed by

McKinney and Amorosi (12) in which the solution was titrated with 0.02 N HCl at controlled pH range with mixed indicator of methyl red and phenolphthalein. The results obtained were lower than that obtained from the other methods. This was probably due to the loss of CO_2 during titration. In method (2) the CO_2 was precipitated as BaCO_3 in excess of 0.1 N Ba(OH)_2 and in method (3) the CO_2 was converted to BaCO_3 in a mixture of 0.1 N NaOH and saturated BaCl_2 solution. In both methods the excess alkali was back titrated with 0.1 N HCl using phenolphthalein as indicator. These last two methods are similar to each other, and the results obtained gave very close check. However, the chemicals involved in method (3) seemed relatively easier to handle. Also this method of analysis was widely employed by a number of investigators on absorption of CO_2 in H_2O , such as Sherwood and Holloway (21). Therefore, the third method was finally chosen in the present study. The details of these three methods, including a comparison with the independent analysis performed by the Analytical and Service Laboratory of the Chemistry Department of Kansas State College are given in Appendix (p. 57).

SUMMARY OF DATA

A total of 35 runs were made for the absorption of carbon dioxide in water in order to evaluate the liquid-film coefficient for the physical absorption in the disc column. Twenty-six runs were retained. Those discarded were the test runs for comparing the method of chemical analysis. The gas rate for the entire ex-

periment was kept at about 10 cu. ft./hr. The liquid rate \bar{V} varied over the range from 100-400 lb./hr. ft. and the liquid temperature range was from 24.8-28.2° C. The data obtained are presented in Table 1. Figure 2 shows the relation of k'_L (corrected to 20° C.) with liquid rate, \bar{V} , which was calculated by dividing the mass rate of liquid by the wetted perimeter for liquid flow. The wetted perimeter was defined as the surface area of the disc divided by its diameter.

Another 30 runs were made for absorption of ammonia in water to establish the gas-film coefficient of the disc column. Seventeen runs were made with varying gas rate. The liquid rate was kept constant at a value of $\bar{V} = 247$ lb./hr. ft. The remainder were made with varying liquid rate over $\bar{V} = 150$ to 400. The concentration of the gas mixture was from 2 to 5 per cent. The liquid temperature range was from 24.5 to 27.5° C. The data obtained are given in Tables 2 and 3. Figure 3 shows the change of the gas-film coefficient with relative velocity of the gas to the surface of the liquid, and Fig. 4 shows the change of the gas-film coefficient with liquid rate. In both cases the coefficients were corrected to 20° C. In the case of varying liquid rate, the coefficient was corrected to a relative velocity of 5.84 ft./sec.

RESULTS AND DISCUSSION

The overall coefficient was calculated by dividing the total mass of carbon dioxide absorbed per hour by the logarithmic driving force based on the liquid concentration. This coefficient was

Table 1. Liquid-film coefficients for absorption of carbon dioxide in water.

Run No.	Water rate : lb./hr.ft.	Water temperature : °C	CO ₂ in : effluent : lb./cu.ft.	CO ₂ absorbed : lb./hr.	Log mean driving force : lb./cu.ft.	k _L : observed	k _L : corrected to 20°C
1	408	25.5	0.0505	0.0420	0.0613	3.11	2.74
2	364	25.5	0.0460	0.0341	0.0642	2.41	2.13
3	322	25.5	0.0465	0.0306	0.0638	2.18	1.92
4	285	25.5	0.0450	0.0261	0.0648	1.83	1.61
5	246	25.0	0.0450	0.0226	0.0662	1.55	1.38
6	213	25.0	0.0435	0.0181	0.0660	1.29	1.15
7	104	28.0	0.0452	0.0096	0.0553	0.787	0.652
8	179	25.9	0.0442	0.0161	0.0649	1.13	1.01
9	148	24.8	0.0462	0.0140	0.0604	1.05	0.920
10	119	27.1	0.0475	0.0115	0.0560	0.934	0.793
11	169	27.4	0.0469	0.0162	0.0555	1.33	1.12
12	195	27.8	0.0472	0.0188	0.0560	1.53	1.29
13	142	27.0	0.0468	0.0135	0.0585	1.05	0.899
14	154	26.8	0.0461	0.0145	0.0580	1.14	0.978
15	128	27.0	0.0518	0.0135	0.0551	1.11	0.956
16	104	26.8	0.0521	0.0110	0.0556	0.899	0.776
17	314	26.0	0.0480	0.0307	0.0609	2.27	2.00
18	368	25.3	0.0480	0.0361	0.0616	2.66	2.36
19	405	25.0	0.0482	0.0398	0.0620	2.92	2.60
20	226	28.1	0.0438	0.0202	0.0564	1.63	1.35
21	292	28.0	0.0463	0.0276	0.0552	2.27	1.89
22	254	27.7	0.0476	0.0247	0.0550	2.04	1.71
23	343	28.2	0.0475	0.0333	0.0538	2.81	2.32
24	364	25.2	0.0520	0.0386	0.0594	2.96	2.63
25	247	24.6	0.0474	0.0238	0.0649	1.67	1.50
26	324	25.9	0.0484	0.0318	0.0604	2.40	2.10

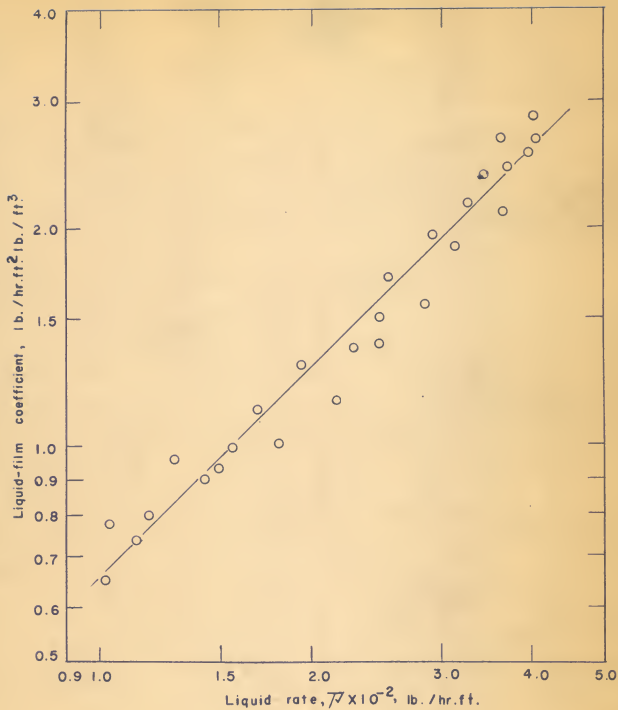


Fig. 2. Liquid-film coefficients for absorption of carbon dioxide in water.

Table 2. Gas-film coefficients for absorption of ammonia in water with variable gas rate.

Run:	Gas velocity: ft./sec.:	Relative velocity: ft./sec.:	Mean water temperature: °C.	Ammonia in effluent: lb./lb.:	Log mean driving force, atm.:	kg. : hr.ft. ² -atm.:	kg. : hr.ft. ² -atm.:	kg. : hr.ft. ² -atm.:
1*	1.98	3.40	25.5	1.14 x 10 ⁻³	2.24 x 10 ⁻²	6.52	6.85	7.28
2†	2.74	3.86	26.4	1.38 x 10 ⁻³	2.17 x 10 ⁻²	7.22	9.05	8.12
3	3.08	4.50	25.5	1.58 x 10 ⁻³	2.42 x 10 ⁻²	8.05	8.44	9.04
4	3.43	4.85	25.5	1.76 x 10 ⁻³	2.69 x 10 ⁻²	8.36	8.76	9.39
5	4.42	5.64	25.8	1.93 x 10 ⁻³	2.70 x 10 ⁻²	8.85	9.33	10.07
6	5.87	7.29	25.5	1.46 x 10 ⁻³	1.70 x 10 ⁻²	11.00	11.50	12.60
7	5.5	6.92	26.4	2.15 x 10 ⁻³	2.78 x 10 ⁻²	9.97	10.55	10.76
8	3.88	5.30	25.9	1.83 x 10 ⁻³	2.55 x 10 ⁻²	8.85	9.30	10.02
9	5.1	6.52	25.1	2.11 x 10 ⁻³	2.71 x 10 ⁻²	9.96	10.42	11.35
10	7.4	8.82	25.5	1.84 x 10 ⁻³	1.97 x 10 ⁻²	12.00	12.6	13.96
11	6.24	7.66	27.4	1.92 x 10 ⁻³	2.24 x 10 ⁻²	11.00	11.71	12.87
12	4.78	6.20	27.5	1.48 x 10 ⁻³	1.99 x 10 ⁻²	9.55	10.18	11.05
13	6.49	7.91	27.7	1.88 x 10 ⁻³	2.17 x 10 ⁻²	11.2	11.95	13.15
14	5.95	7.37	24.8	2.04 x 10 ⁻³	2.54 x 10 ⁻²	10.3	10.73	11.72
15	6.67	8.09	24.7	2.01 x 10 ⁻³	2.30 x 10 ⁻²	11.2	11.68	12.86
16	4.42	5.84	24.5	1.94 x 10 ⁻³	2.60 x 10 ⁻²	9.22	9.6	10.4
17	5.5	6.92	26.0	2.10 x 10 ⁻³	2.80 x 10 ⁻²	9.67	10.20	11.08

Liquid rate was kept constant at = 247 lb./hr.ft.

The free space with liquid flowing was taken to be 89% at this liquid rate.

*These two runs were made with N₂ as inert gas.

Table 3. Gas-film coefficients for absorption of ammonia in water, with variable liquid rate.

Run:	Water rate No.:lb./hr.ft. ² :	Relative velocity: ft./sec.:	Mean temperature: °C.:	Ammonia in effluent: lb./lb.:	Log mean driving force, atm.:	Ammonia in water: lb.:	Gas-film coefficient: K _G : hr.ft. ² ·atm. ⁻¹ ·sec. ⁻¹ :	Gas-film coefficient: K _G : hr.ft. ² ·atm. ⁻¹ ·sec. ⁻¹ corrected to 20°C:	Gas-film coefficient: K _G : hr.ft. ² ·atm. ⁻¹ ·sec. ⁻¹ corrected to 20°C:
1	199	4.75	27.5	1.55 x 10 ³	1.83 x 10 ⁻²	8.75	9.33	10.22	11.62
2	220	4.82	27.4	1.24 x 10 ³	1.49 x 10 ⁻²	8.95	9.55	10.41	11.73
3	360	5.34	27.4	1.02 x 10 ³	1.64 x 10 ⁻²	11.45	12.2	13.02	13.72
4	285	5.08	25.0	1.22 x 10 ³	1.71 x 10 ⁻²	10.52	11.0	12.02	13.10
5	185	4.69	25.5	1.63 x 10 ³	1.86 x 10 ⁻²	8.5	8.91	9.81	11.25
6	378	5.24	25.6	0.99 x 10 ³	1.63 x 10 ⁻²	11.65	12.22	13.05	13.94
7	255	4.97	25.5	1.33 x 10 ³	1.69 x 10 ⁻²	10.08	10.57	11.48	12.67
8	244	4.93	25.4	1.36 x 10 ³	1.78 x 10 ⁻²	9.7	10.15	11.04	12.25
9	155	4.55	27.5	1.68 x 10 ³	1.70 x 10 ⁻²	8.11	9.39	9.67	11.30
10	300	5.33	26.7	1.37 x 10 ³	1.93 x 10 ⁻²	10.94	11.6	12.53	13.22
11	395	5.65	25.3	1.12 x 10 ³	1.82 x 10 ⁻²	12.45	13.02	13.90	14.12
12	337	5.26	26.2	1.06 x 10 ³	1.64 x 10 ⁻²	11.11	11.75	12.60	13.40
13	320	5.20	26.1	1.11 x 10 ³	1.71 x 10 ⁻²	10.70	11.20	12.12	13.00

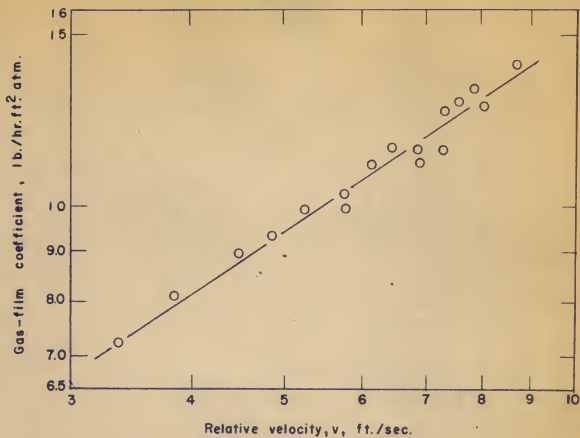


Fig. 3. Effect of gas velocity on gas-film coefficient for absorption of ammonia in water.

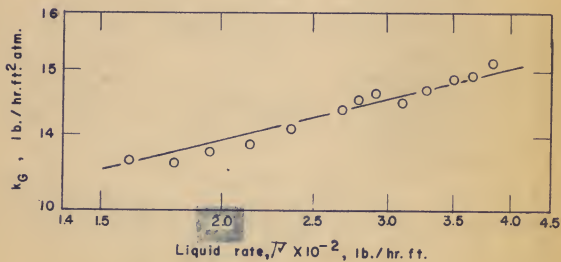


Fig. 4. Effect of liquid rate on gas-film coefficient for absorption of ammonia in water.

taken as the liquid-film coefficient since the solubility of carbon dioxide in water is small and since the gas phase resistance for absorption of carbon dioxide is not appreciable as verified by Sherwood and Holloway (22). All the observed coefficients were corrected to a standard temperature of 20° C. by means of the relationship:

$$k_L' \propto e^{0.023T} \quad (14)$$

obtained by Sherwood and Holloway (22). In Fig. 2, a plot of k_L' vs. \mathcal{P} shows considerable scattering, but there still appears a trend that they can be represented by a single straight line. By employing the method of least squares, the data are correlated by the equation:

$$k_L' = 0.0075\mathcal{P}^{0.97} \text{ lb./hr. ft.}^2 \text{ lb./ft.}^3 \text{ at } 20^\circ \text{ C.} \quad (15)$$

The slope of the straight line, being nearly unity, is much larger than those reported in the literature. Sherwood and Holloway (22) measuring the liquid-film coefficient for various kind of packing, found that k_L' is proportional to \mathcal{P}^n , where n varied from 0.54 to 0.78. Stephens and Morris (24), in their experiment of absorption of carbon dioxide in water by a ceramic disc column, gave a value of $n = 0.7$. Roper (18) using a carbon disc column gave the same value of "n" as Stephens and Morris. The larger value of the slope, or the exponential "n", means that the liquid rate affects the liquid-film transfer much more than those observed by the various investigators mentioned above.

Also the concentration of carbon dioxide in the outlet liquid was found to increase slightly with the liquid rate, while Stephen

and Morris' data showed a decrease with increasing liquid rate. A plot of the outlet concentration of carbon dioxide from the author's data and those of Stephen and Morris' is shown in Fig. 5.

If we consider alone the duration of the contact time between the gas and liquid streams, then the exit liquid concentration should decrease as the liquid rate increases. However, there is another factor which would have the opposite effect. That is, as the liquid rate increases, the liquid stream would become more turbulent and afford better mixing below the liquid surface as well as more "fresh" surfaces available for absorption.

In the light of Danckwerts mechanism of liquid film (2), the capacity for absorption is proportional to the number of fresh surfaces exposed to the gas. The rate of the creation of fresh surfaces is, in turn, a function of turbulence and the rate of the liquid flowing from one disc to the next. By visual inspection of the flow pattern in the disc column, it was observed that the disc surfaces could not be completely wetted until the liquid rate, had reached 150 lb./hr. ft. and when was further increased, the turbulence of the liquid layer became increasingly vigorous. Also at low flow rate, the liquid tended to channel along the edge of the disc. The excessive smoothness and the poor wetting characteristics of the disc surface suggest an explanation for the apparent contradictions with the literature data: (1) In the present column, the packing was not completely wetted until a critical flow rate had been reached; further increase in rate produced more turbulence and consequently higher absorption rate and higher outlet concentration of CO_2 in liquid. Roper used "carbon" discs

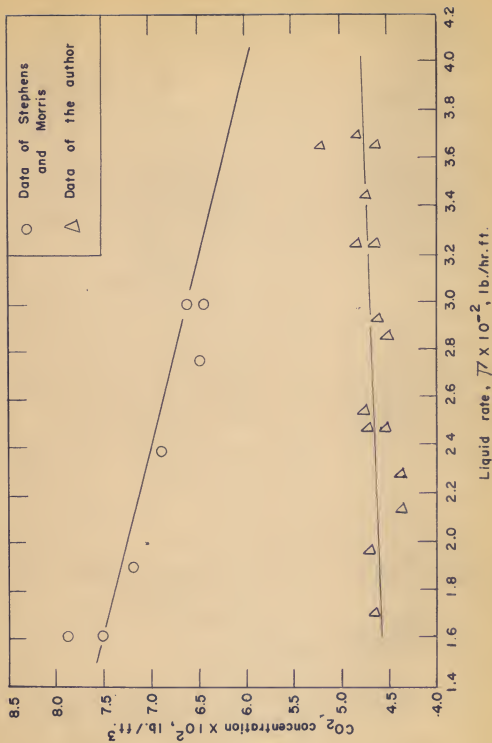


Fig. 5. Plot of exit carbon dioxide concentration vs. liquid rate, \bar{V} .

and Stephen and Morris used "ceramic" discs. In either case, the surface roughness was presumably higher so that at the same flow rates studied a maximum turbulence was already attained. Therefore, the outlet liquid concentration did not increase with the rate. (2) The pronounced influence of the rate upon the liquid film coefficient by virtue of the increased turbulence was also manifested by the high value of the exponential ($n = 0.97$) in equation (14). (3) The excessive smoothness of the present discs may also account for the comparatively low value of the liquid film coefficient.

To test further the validity of these explanations, a series of absorption runs should be made keeping the roughness of the disc surface as the sole variable. That is, to use a series of packings of increasing roughness in subsequent runs operating in the same temperature, pressure, and flow ranges. According to the reasoning mentioned above, the following correlation should result: First, plotting $\log k_L$ versus $\log \mathcal{V}$, the straight line for the smooth surface discs should have a slope close to unity; as the roughness increases, the line should displace to a higher position but it should have a smaller slope. Then, plotting the outlet liquid concentration versus the liquid rate, the line for the smooth surface discs should have a positive slope; as the roughness increases, the lines should displace to a higher position and the slope should decrease until it becomes negative. These predictions are shown graphically in Fig. 6 and Fig. 7.

The liquid film coefficient of the present column ranges from 0.9 to 2.7 lb./hr. ft.² (lb./ft.³). Under similar operating



Fig. 6. Prediction of the relationship between k_L and $\sqrt{\omega}$ for different degree of roughness of disc surface.

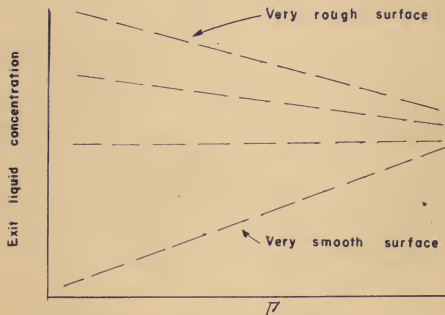


Fig. 7. Prediction of the relationship between the exit liquid concentration and $\sqrt{\omega}$ for different degree of roughness of disc surface.

conditions, Stephen and Morris' column had a k_L^1 value between 1.5 to 3.2. In addition to the surface roughness and wetting characteristics, the variation in the disc dimensions may also have contributed to this difference in column performance. For absorption of other systems with the same apparatus, the influence factor of the column itself should be the same. The correlation based on the present experiment, $k_L^1 \propto \mathcal{P}^{0.97}$ should apply. A dimensional equation similar to that obtained by Sherwood and Holloway (22) from experiments with packed towers is assumed to be applicable for estimating the liquid film coefficients for physical absorption of other systems at any other condition.

$$\frac{k'_L}{D} = a \left(\frac{4\mathcal{P}}{\mu} \right)^m \left(\frac{\mu}{\rho D} \right)^n \quad \text{ft.}^{-1} \quad (16)$$

Since $k_L^1 \propto \mathcal{P}^{0.97}$, therefore, m in the above equation should take a value of 0.97. n in this case was taken to be 0.5, since, according to Higbie (8), k_L^1 is proportional to the square root of the diffusivity, D , and according to Sherwood and Holloway (22), k_L^1 is proportional to the 0.5 power of the Schmidt group. The constant "a" was calculated by substituting the values of the dimensionless groups and comparing the equation (15). The resulting equation is:

$$\frac{k'_L}{D} = 3.08 \left(\frac{4\mathcal{P}}{\mu} \right)^{0.97} \left(\frac{\mu}{\rho D} \right)^{0.5} \quad \text{ft.}^{-1} \quad (17)$$

The calculation is shown in Appendix (p. 62).

The overall coefficients for absorption of ammonia in water were calculated from the weight of ammonia absorbed per hour and the logarithmic mean driving force in terms of solute partial

pressure (Appendix, p. 62). The coefficients obtained were corrected to a standard liquid temperature of 20° C. by the method of Molstad, et al (13). Their equation for temperature correction was rearranged by the author as follows:

$$K_G \propto 24.3 - 0.175t \quad (18)$$

The liquid-film coefficient was then calculated by equation (17) and corrected to a liquid temperature of 20° C. The value of diffusivity was taken from p. 540, Perry's Handbook (15). The viscosity and density were assumed to be those of pure water because of the low concentration of the exit solution. Then the gas-film coefficient were calculated by the equation

$$\frac{1}{K_G} = \frac{1}{k_G} + \frac{H}{k_L} \quad (19)$$

The Henry's law constant were obtained by means of the equation derived by Kowlke et al (11). A plot of the gas-film coefficient against the relative velocity is shown in Fig. 3. They are well correlated by the equation:

$$k_G = 3.32 v^{0.65} \quad (20)$$

This result checks closely with that obtained by Stephens and Morris (24). They found in their disc column that

$$k_G \propto v^{0.67} \quad (21)$$

The coefficients obtained were about 100 per cent lower than those of Stephens and Morris. Figure 4 shows the influence of liquid rate upon k_G . The line exhibits the same trend indicated by Stephens and Morris' data, and again, the liquid flow has much more effect on the k_G for the present column than that of Stephens and Morris. The correlation of the present data gives

$$k_G = 2.96 \mathcal{V}^{0.26} \quad (22)$$

While that of Stephens and Morris gives

$$k_G = 11.1 \mathcal{V}^{0.13} \quad (23)$$

This is consistent with the observation from the CO_2 runs that the liquid rate has much more effect upon the performance of the present disc column than that employed by Stephens and Morris.

For extrapolation of this result to another system at other conditions, a dimensional equation was developed. The equation was considered to take the following form:

$$\frac{k_G P_{GM}}{V_{PL}} = b \left(\frac{v_{DP}}{\mu} \right)^{-m} \left(\frac{\mu}{P_D} \right)^{-n} \quad (24)$$

which is the general correlation for wetted-wall column. The exponent m is equal to $1 - 0.65 = 0.35$, since

$$k_G \propto \mathcal{V}^{0.65} \quad (25)$$

and the value of $n = 0.56$ was selected, based on Gilliland and Sherwood's (4) conclusion. Inserting the physical constants in equation (24), the constant "b" for constant liquid rate and a relative velocity of 5.84 ft./sec., which was the common condition to Fig. 3 and Fig. 4, was found to be 0.12. The coefficient is proportional to 0.26 power of the liquid rate. Incorporating these constants, the final correlation becomes

$$\frac{k_G P_{GM}}{V_{PL}} = 0.034 \mathcal{V}^{0.26} \left(\frac{v_{DP}}{\mu} \right)^{-0.35} \left(\frac{\mu}{P_D} \right)^{-0.56} \quad (26)$$

The detailed computation is shown in Appendix, p.66 .

CONCLUSION

The results of the present work and the conclusions derived therefrom are summarized as follows:

1. A disc column with its necessary accessories has been constructed and calibrated. The operational and analytical procedures have been tested.

2. The liquid-film coefficients, k_L^i , of the column ranging between 0.7 and 2.7 lb./hr. ft.² lb./ft.³ were determined in a series of experiments of the absorption of CO₂ in water. k_L^i was found to be proportional to the 0.97 power of the liquid rate, \mathcal{V} , over the range of \mathcal{V} from 100 to 400 lb./hr. ft. The following correlation is proposed to include the other liquid properties such as viscosity, density, and diffusivity:

$$\frac{k_L^i}{D} = 3.03 \left(\frac{4\mathcal{V}}{\mu} \right)^{0.97} \left(\frac{\mu}{\rho D} \right)^{0.5} \text{ ft.}^{-1}$$

3. The gas-film coefficients, k_G , of the column ranging between 7 to 13 lb./hr. ft.² atm. were determined in a series of experiments of absorption of dilute NH₃ in water. k_G was found to be proportional to the 0.65 power of the "relative velocity" between the gas and liquid at a constant \mathcal{V} of 247 lb./hr. ft. and to the 0.26 power of \mathcal{V} over the range of \mathcal{V} from 150 to 400. The following correlation has been developed:

$$\frac{k_G \rho_a M}{\nu \rho_a} = 0.034 \mathcal{V}^{0.26} \left(\frac{\nu \rho}{\mu} \right)^{-0.35} \left(\frac{\mu}{\rho D} \right)^{-0.56}$$

4. The performance of the column is considered satisfactory for the use in further investigations on the absorption processes

with simultaneous chemical reaction. For an unknown gas-liquid system, the overall absorption coefficient can be experimentally determined. Then the liquid-film coefficient, k_L , can be computed by eliminating the k_G value predicted by the correlation in 3 above. The ratio between k_L , the liquid-film coefficient with chemical reaction thus computed, and k_L^i , the liquid-film coefficient of pure physical absorption as predicted by the correlation in 2, may be used as a guide in the actual column design where the value of k_L^i for the packing is known but the knowledge of k_L is completely lacking. However, a more useful function of this column would be for the study of the influence of liquid concentration and gas partial pressure as well as the flow rates upon k_L . Such information can be used to establish the combined mechanism of diffusion and chemical reaction in the absorption process.

ACKNOWLEDGMENTS

The author wishes to express his gratitude to the Kansas State College Engineering Experiment Station for the financial assistance which made this research possible, and to:

Drs. S. L. Wang and Henry T. Ward for their advice and encouragement during the course of this work;

Mr. Chi Tien, Graduate Assistant, and Mr. George Ghahramanian, a senior student, both of the Department of Chemical Engineering, Kansas State College, for their assistance.

BIBLIOGRAPHY

- (1) Carlson, H. C., *Ind. Eng. Chem.* 41, 12, 1949.
- (2) Danckwerts, P. V., *Ind. Eng. Chem.* 43, 1460, 1951.
- (3) Furnas, C. C., and F. Bellinger, *Trans. Am. Inst. Chem. Engrs.* 34, 264, 1938.
- (4) Gilliland, E. R., and T. K. Sherwood, *Ind. Chem. Eng.* 26, 516, 1934.
- (5) Grimley, S. S., *Trans. Inst. Chem. Engrs. (London)*, 23, 228, 1945.
- (6) Hatta, S., *Techol. Repts., Tohoku Imp. Univ.*, 8.1, 1928-29. Original not seen. Reported by Sherwood and Pigford (20).
- (7) Hatta, S., *Techol. Repts., Tohoku Imp. Univ.*, 10, 119, 1932. Original not seen. Reported by Sherwood and Pigford (20).
- (8) Higbie, R., *Trans. Am. Inst. Chem. Engrs.* 31, 365, 1935.
- (9) Hougen, O. A., and K. M. Watson, *Chemical Process Principles, Vol. I*, pp. 100. New York: John Wiley and Sons.
- (10) Jenny, F. J., *Thesis in Chemical Engineering, M. I. T.* Original not seen. Reported by Sherwood and Pigford (20).
- (11) Kowalke, O. L., O. A. Hougen, and K. M. Watson, *Bull. Univ. Wis. Eng. Expt. Sta.* 68, June, 1925.
- (12) McKinney, D. S., and A. M. Amorosi, *Ind. Eng. Chem., Anal. Ed.*, 16, 315, 1944.
- (13) Molstad, M. C., J. F. McKinney, and R. G. Abbey, *Trans. Am. Inst. Chem. Engrs.* 39, 605, 1943.
- (14) Payne, J. W., and B. F. Dodge, *Ind. Eng. Chem.* 24, 630, 1932.
- (15) Perry, J. H., *Chemical Engineers' Handbook*, 3rd Ed., New York: McGraw-Hill Co., 1950.
- (16) Pigford, R. L., *Ind. Eng. Chem.* 42, 17, 1951.
- (17) Pozin, M. E., *J. Applied Chem. (U. S. S. R.)*, 20, 345-352, 353-359, 963-975, 754-61, 1947. Original not seen. Reported by Carlson (1).

- (18) Roper, G. H., Chemical Engineering Science (London) 2, 18, 1953.
- (19) Scott, W. W., Standard Methods of Chemical Analysis, 5th Ed., pp. 2270, New York: D. Van Nostrand Co.
- (20) Sherwood, T. K., and R. L. Pigford, Absorption and Extraction, New York: McGraw-Hill Co., 1952.
- (21) Sherwood, T. K., and F. A. L. Holloway, Trans. Am. Inst. Chem. Engrs., 36, 21, 1940.
- (22) Sherwood, T. K., and F. A. L. Holloway, Trans. Am. Inst. Chem. Engrs., 36, 39, 1940.
- (23) Spector, N. A., and B. F. Dodge, Trans. Am. Inst. Chem. Engrs., 42, 827, 1946.
- (24) Stephens, E. J., and G. A. Morris, Chem. Eng. Prog. 47, 232, 1951.
- (25) Tepe, T. B., and B. F. Dodge, Trans. Am. Inst. Chem. Engrs. 39, 255, 1943.
- (26) Theory of the Flowrator, Catalog Section 98-A, Fisher and Porter Company, Hatboro, Pennsylvania.
- (27) The F & P Tri-Flat (Low flow rate) Variable-Area Flow meter Handbook, Fisher and Porter Company, Hatboro, Pennsylvania.
- (28) Treadwell, F. P., and W. T. Hall, Analytical Chemistry, Vol. II, p. 520, New York: John Wiley and Sons, Inc.
- (29) Turken, E. Ya., J. Applied Chem. (U. S. S. R.), 21, 927, 1948. Original not seen. Reported by Pigford (14).
- (30) Van Krevelin, D. W., and T. J. Holtzger, Chem. Eng. Prog. 44, 529, 1948.
- (31) Whitesman, W. G., and D. S. David, Ind. Eng. Chem. 16, 1233, 1924.

APPENDIX

Calibration of Flowmeters

The Brooks rotameters were calibrated for CO₂ gas and for N₂ gas against a wet test meter of the Precision Scientific Company. Before the calibration was made, the wet test meter itself was checked by displacement of water to test its accuracy. The rotameter to be calibrated was set in series with the wet test meter. Gas first passed through the rotameter, then entered the wet test meter and exit to atmosphere. The water in the wet test meter was saturated by passing the gas through for about two hours or more before each series of calibration runs was started.

The flow was controlled by a $\frac{1}{4}$ -inch stainless steel needle valve. The volume as indicated by the wet test meter and the pressures and temperatures at the downstream of the rotameter and at the wet test meter were recorded. Calculations were made to present the data as flow rates of gas in cu. ft./min., at 0° C. and 760 mm. Hg. An example from the calibration runs is given as follows:

Rotameter # 4(4-15-2), CO₂, Monel Float

Data: Rotameter reading, 9.00
 Gas temperature at rotameter, 92.5° F.
 Atmospheric pressure, 730.12 mm. Hg (corrected)
 Gas pressure at rotameter, 83 mm. H₂O above atmospheric
 Time of run 252.5 sec.
 Gas flow 0.5 cu. ft. as read on the wet test meter
 Gas pressure at wet test meter 0 psi
 Gas temperature at wet test meter 91.0° F.

Gas flow rate at 0° C. and 760 mm. hg is (assuming gas law holds at this temperature and pressure)

$$\begin{aligned}
 V_2 &= \frac{P_1 V_1 t_2}{P_2 t_1} \\
 &= \frac{730.12 \times 0.5 \times 60 \times 492}{760 \times 551 \times 252.5} \\
 &= 0.102 \text{ cu. ft./min.}
 \end{aligned}$$

It will be noted that this is the flow rate in cu. ft. CO₂/min. measured at 0° C. and 760 mm. Hg. Actually, the gas is flowing through the rotameter under a pressure of 83 mm. H₂O above atmospheric and 92.5° F. This will be the approximate pressure and temperature in actual runs of absorption operation. However, if there is much difference in pressure and temperature between the operation condition and the calibration condition, the rotameter readings must be corrected by (26)

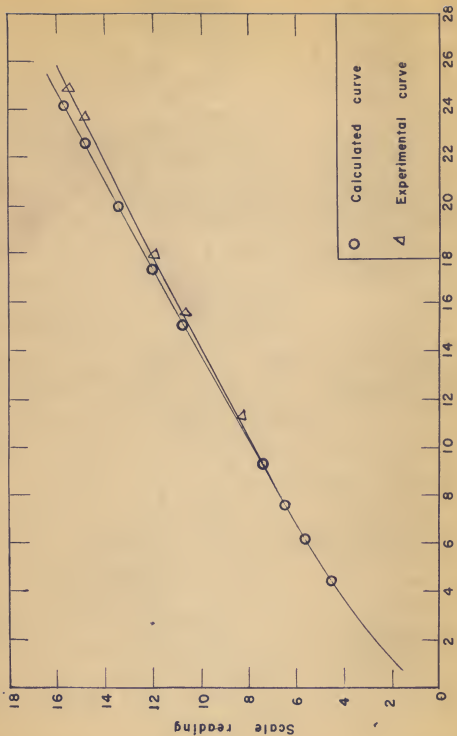
$$Q_2 = Q_1 \times \sqrt{\frac{P_2 T_1}{P_1 T_2}}$$

Where $Q_1, 2$ = flow rate at calibration and operation conditions, respectively

$P_1, 2$ = pressure at calibration run and operation run, respectively

$T_1, 2$ = temperature at calibration run and operation run, respectively.

Calibration curves of scale reading against flow rate for the F & P Tri-Flat Flowrators were calculated by the method and procedure furnished by the manufacturer (27). In order to check the accuracy of the calculated curve, experimental calibrations were also made for N₂ using the already calibrated Brook's rotameter as a standard. The experimental and the calculated calibration curves were plotted in Fig. 8 for comparison. It was shown from the plot that the two curves were almost superimposed. Thus, the accuracy of the calculated calibration curves was considered satisfactory.



Flow rate of nitrogen gas, $\text{C.F.M.} \times 10^2$ at 14.7 lb./in.^2 , 70°F.

Fig. 8. Calibration curves for F.B.P. Flowrate No. 2 F— 1 / 4— 16— 5.

Evaluation of Chemical Analysis

During the test runs, three methods of chemical analysis of CO_2 in H_2O were compared.

1. Determination of Carbon Dioxide in H_2O . This method was proposed by McKinney and Amorosi (12) for determination of CO_2 in industrial water. The procedure of this method is given as below:

(1) Select two 250 ml Erlenmeyer flasks. Place 100 ml of pH 8.5 buffer solution in one and 100 ml of pH 5 in the other. To each, add 0.4 ml of mixed indicator (methyl red and phenolphthalein were used in the test runs) and cork the flasks.

(2) In the third flask, add 0.4 ml of mixed indicator to 100 ml of the water to be tested.

(3) Titrate the sample to pH 8.5 by using standard NaOH (usually 0.02 N). If the sample is more alkali than pH 8.5, standard HCl will be used in this procedure. Record the volume required as V_{1x} if NaOH is used.

(4) Titrate the sample from pH 8.5 to pH 5 with HCl. Record the volume used as V_1 .

(5) Acidify by adding 20 per cent more of the acid than was required for V_1 . Boil the solution vigorously for two minutes over a strong flame.

(6) Cool the flask rapidly in running water to room temperature. Add NaOH until the pH is 8.5, and record the volume of base required as V_{2x} . Now titrate the sample from pH 8.5 to pH 5 with HCl, and record the volume of acid used as V_2 .

For correcting the CO_2 content in NaOH, the following proce-

ture was proposed by McKinney:

(1) To 80 ml of CO_2 free distilled H_2O , add 0.4 ml of mixed indicator and sufficient $\text{N}10\text{H}$ to bring the pH to 8.5. Then titrate to pH 5 using H_g . Let A be the volume of acid used. Add immediately 20 ml of NaOH and again titrate with acid, noting the volume required to change the pH from 8.5 to 5. Let this volume be B. Disregard the volume of NaOH required to titrate the 20 ml of base to pH 8.5. The correction factor is then:

$$\frac{B - A}{20} = X$$

The carbon dioxide in the sample is calculated by the following formula:

$$\text{CO}_2 \text{ (ppm)} = K \times \frac{1000}{V_s} \times N \left(V_1 - V_{1x}X \right) - \left(V_2 - V_{2x}X \right)$$

Where $K = 45.56$, if titration from pH 8.5 to 5 is used,

$K = 43.95$, if titration from pH 9 to 5 is used,

V_s = Sample volume in ml (usually 100 ml),

N = Normality of HCl solution,

V_1, V_2 = ml of acid required to titrate respectively, unboiled and boiled sample from pH 8.5 to 5.0, (or pH 9 to 5 if this end pt. are used),

V_{1x}, V_{2x} = ml of base used to adjust unboiled and boiled sample, respectively, to pH 8.5 or 9,

V = ml of acid required to titrate CO_2 in 1 ml of base from pH 8.5 - 5 (pH 9.5).

(2) Precipitate the CO_2 as CO_3 in excess 0.1N Ba(OH)_2 . Then titrate the excess of Ba(OH)_2 by 0.1 N HCl with phenolphthalein indicator.

(3) Precipitate the CO_2 as BaCO_3 in a mixture of 0.1 NaOH

and saturated $BaCl_2$. The excess of NaOH was then titrated with 0.1 HCl to a phenolphthalein end point.

A set of analysis data for the same sample by three methods are given as follows:

Table 4. Data of Method 1.

Sample No. :	V_1	V_{1x}	V_2	V_{2x}	X	CO_2 p.p.m.
1	15.94	15.20	1.16	4.19	0.0525	255
2	14.19	12.78	1.63	2.29	"	217
3	14.90	13.15	0.98	4.19	"	241
4	15.84	15.20	1.02	4.00	"	256
5	17.32	16.55	1.10	4.38	"	280

$$A = 0.2, B = 1.25, X = \frac{B - A}{20} = 0.0525$$

Reagents used = 0.02 N. NaOH, 0.02 N. HCl, mixed indicator of methyl red and phenolphthalein. Volume of sample = 50 ml.

Table 5. Data of Method 2.

Sample No. :	0.1N. $Ba(OH)_2$	0.1NHCl	0.1N $Ba(OH)_2$	CO_2
:	:	:	Consumed	ppm
1a	15.32	2.70	12.62	555
2a	13.50	1.14	12.36	544
3a	13.66	1.24	12.42	547
4a	13.52	1.22	12.30	541
5a	13.57	1.13	12.44	547

Volume of sample 50 cc.

Table 6. Data of Method 3.

Sample No. :	0.1N NaOH	0.1NHCl	0.1N NaOH	CO_2
:	:	:	Consumed	ppm
1b	14.0	1.25	12.75	561
2b	14.0	1.45	12.55	552
3b	14.0	1.40	12.6	555
4b	14.0	1.55	12.45	548
5b	14.0	1.43	12.57	553

Volume of sample 50 cc. Saturated $BaCl_2$ 10cc.

Dry-bulb temperature of the exit gas = 82.8°F.

Humidity of exit gas (9) = 0.0345 $\frac{\text{mole of H}_2\text{O}}{\text{mole of CO}_2}$

Concentration of CO₂ in inlet water = 0

Concentration of CO₂ in outlet water = 0.0462 lb./cu.ft.

Total pressure at inlet = partial carbon dioxide at inlet = 737.93 + 4.89 = 742.82 mm Hg = 0.977 atm.

Total pressure at outlet = 737.93 + 2.76 = 740.69 mm Hg

Partial pressure of H₂O at outlet = $\frac{0.0345}{1.0345} \times 740.69$

= 24.66 mm Hg.

Partial pressure of CO₂ at outlet = 740.69 - 24.66

= 716.03 = 0.942 atm.

The equilibrium concentration of carbon dioxide at the interface at the ends of the column is

$$x_1^* = \frac{0.977}{1,795} = 0.000544 \frac{\text{lb-mole of CO}_2}{\text{lb-mole of solution}}$$

$$X_1^* = 0.0827 \frac{\text{lb. of CO}_2}{\text{cu.ft. of solution}}$$

$$x_2^* = \frac{0.942}{1,795} = 0.000525$$

$$X_2^* = 0.0796$$

$$X_1 = 0.0462$$

$$X_2 = 0$$

$$(\Delta X)_{lm} = \frac{(0.0827 - 0.0462) - 0.0796}{1.1 \frac{0.0827 - 0.0462}{0.0796}} = 0.0552 \text{ lb./ft.}^3$$

Carbon dioxide absorbed per hour = 0.0276 lbs.

$$(k_L')_{\text{obs.}} = \frac{0.0276}{0.22 \times 0.0552} = 2.27$$

Since $k_L' \propto e^{0.023t}$

$$(k_L')_{20^\circ} = (k_L')_{\text{obs.}} \frac{e^{0.023 \times 20}}{e^{0.023 \times 27.9}} = 1.89 \text{ lb./hr. ft.}^2 \text{ lb./ft.}^3$$

2. Evaluation of the constants for the empirical equation

By employing the method of least squares to correlate the experimental results, the following equation was obtained

$$k_L' = 0.0075 P^{0.97} \quad (15)$$

An equation of the following form was selected

$$\frac{k_L'}{D} = a \left(\frac{4P}{\mu} \right)^m \left(\frac{\mu}{\rho D} \right)^n \quad \text{ft.}^{-1} \quad (16)$$

Let $n = 0.5$, $m = 0.97$. Equation became

$$\frac{k_L'}{D} = a \left(\frac{4P}{\mu} \right)^{0.97} \left(\frac{\mu}{\rho D} \right)^{0.5} \quad \text{ft.}^{-1} \quad (16')$$

Comparing equation (16') to equation (15), the following relationship resulted

$$0.0075 = aD \left(\frac{4}{\mu} \right)^{0.97} \left(\frac{\mu}{\rho D} \right)^{0.5} \quad (16'')$$

at 20°C

$$D = 1.5 \times 10^{-5} \text{ cm.}^2/\text{sec.}$$

$$= 5.81 \times 10^{-5} \text{ ft.}^2/\text{sec.}$$

$$\mu = 1.005 \text{ centipoise}$$

$$= 2.43 \text{ lb./hr.ft.}$$

$$\frac{\mu}{\rho D} = 670 \text{ (dimensionless)}$$

$$a = 0.0075 / [5.81 \times 10^{-5} \left(\frac{4}{\mu} \right)^{0.97} \left(\frac{\mu}{\rho D} \right)^{0.5}]$$

$$= 3.08$$

Therefore, the final equation is

$$\frac{k_L'}{D} = 3.08 \left(\frac{4P}{\mu} \right)^{0.97} \left(\frac{\mu}{\rho D} \right)^{0.5} \quad \text{ft.}^{-1} \quad (17)$$

B. Absorption of Ammonia in Water

1. Calculation of the overall transfer coefficient

Run No. 3 of absorption of ammonia in water with varying liquid rate.

Observed data:

Atmospheric pressure (corrected) = 728.88 mm Hg.

Room temperature = 24.5°C.

Mean liquid temperature = 27.4°C. = 541.2°R.

Air rate = G = 4.1 lb./hr.

Ammonia rate = 0.0686 lb./hr.

Water rate, L = 45.8 lb./hr. = 360 lb./hr.ft.

Concentration of ammonia in inlet liquid, $X_2 = 0$

Concentration of ammonia in outlet liquid, $X_1 = 0.00102$
lb. of NH_3 /lb. of solution

Inlet gas concentration, $Y_1 = \frac{0.0686}{4.1} = 0.0167 \frac{\text{lb. of } \text{NH}_3}{\text{lb. of air}}$

Outlet gas concentration, Y_2 was found by material balance.

Since

$$L(X_1 - X_2) = G(Y_1 - Y_2)$$

for dilute solution, the outlet gas concentration

$$Y_2 = Y_1 - \frac{L}{G} X_1$$

$$= 0.0053 \text{ lb. of } \text{NH}_3/\text{lb. of air}$$

Manometer reading at inlet of the column = 58 mm Hg.

Total pressure at inlet of the column = 728.88 + 58
= 786.88 mm Hg.

Manometer reading at outlet of the column = 19 mm Hg.

Total pressure at outlet of the column = 728.88 + 19
= 747.88 mm Hg.

Partial pressure of ammonia at inlet

$$= \frac{(0.0686/17)}{(0.0686/17 + (4.1/29))} 786.88$$

$$= 21.8 \text{ mm Hg.}$$

Partial pressure of ammonia at outlet =

$$\frac{(0.0053/17)}{(0.0053/17) + (1/29)} 747.88 = 6.7 \text{ mm Hg.}$$

The equilibrium pressure of the solute gas was calculated by the following equation

$$\log \frac{p'}{C} = 4.699 - \frac{3460}{T^{\circ}\text{R}}$$

where p' = equilibrium pressure of ammonia, atm.

c = concentration of ammonia in molarity

$$= X \times \frac{1000}{17}$$

$$\log \frac{(p')}{(c)_1} = -1.694 = \bar{2}.306$$

$$\frac{(p')}{(c)_1} = 0.02023$$

$$p_1' = (0.00102) \left(\frac{1000}{17} \right) (0.02023) (760) = 0.92 \text{ mm Hg.}$$

$$p_2' = 0, \text{ since } X_2 = 0.$$

$$(\Delta p)_{lm} = \frac{(21.8 - 0.92) - 6.7}{\ln \frac{21.8 - 0.92}{6.7}} = 12.5 \text{ mmHg} = 1.64 \times 10^{-2} \text{ atm.}$$

$$K_G = \frac{G(Y_1 - Y_2)}{A (\Delta p)_{lm}}$$

where A = absorption surface, for this liquid rate, it was found to be 0.248 ft.^2 . The method of calculation is given on p. 63.

$$K_G = \frac{4.1 \times 0.0114}{0.248 \times 0.0164} = 11.45 \text{ lb./hr.ft.}^2 \text{ atm.}$$

Since

$$K_G \propto 24.3 - 0.175 t$$

K_G at 20°C is

$$11.45 \frac{24.3 - 0.175 \times 20}{24.3 - 0.175 \times 27.4} = 12.2 \text{ lb./hr.ft.}^2 \text{ atm.}$$

2. Calculation of the gas-film coefficient

The gas-film coefficient is calculated by the equation

$$\frac{1}{K_G} = \frac{1}{k_G} + \frac{H}{k_L}$$

The value of H was calculated by the following equation (11)

$$\log \frac{p'}{c} = 4.699 - \frac{3.460}{T^{\circ}R}$$

$$\begin{aligned} H = \frac{p'}{c} &= 0.02023 \text{ atm./}(\text{g-mole of NH}_3/\text{1,000 g. of H}_2\text{O}) \\ &= \frac{0.02023 \times 1,000}{17} \text{ atm./}(\text{lb. of NH}_3/\text{lb. of H}_2\text{O}) \\ &= \frac{0.02023 \times 1,000}{17 \times 62.4} \text{ atm./}(\text{lb. of NH}_3/\text{cu.ft. of H}_2\text{O}) \\ &= 0.013 \text{ atm./}(\text{lb. of NH}_3/\text{cu.ft. of H}_2\text{O}) \end{aligned}$$

k'_L was estimated by using equation (17)

$$\frac{k'_L}{D} = 1.08 \left(\frac{\mathcal{V}}{\mu} \right)^{0.97} \left(\frac{\mu}{\rho D} \right)^{0.5} \text{ ft.}^{-1}$$

where $D = 6.82 \times 10^{-5} \text{ ft.}^2/\text{hr.}$ (p. 540, Perry's Handbook)

$$\frac{\mu}{\rho D} = 570$$

$\mu = 0.8545 \text{ centipoise}$ (p. 374, Perry's Handbook)

$\mathcal{V} = 360 \text{ lb./hr.ft.}$

$$k'_L = 2.98$$

Corrected k'_L to 20°C by the relation

$$k'_L \propto e^{0.023 T}$$

$$(k'_L)_{20^{\circ}\text{C}} = 2.521$$

$$\frac{H}{k'_L} = 0.00525$$

$$\frac{1}{k_G} = 0.0820$$

$$\frac{1}{k_G} = 0.0820 - 0.00525 = 0.0768$$

$$k_G = 13.02 \text{ lb./hr.ft.}^2\text{atm.}$$

The surface velocity of this liquid rate was

$$v_1 = 1.825 \text{ ft./sec.}$$

The method of estimating the liquid surface velocity if given on p. 63. The gas linear velocity was

$$v_g = 3.52 \text{ ft./sec.}$$

The relative velocity to the liquid surface was

$$3.52 + 1.825 = 5.345 \text{ ft./sec.}$$

The correction of k_G to a relative velocity of 5.84 ft./sec.

was made by means of Fig. 3. From Fig. 3, k_G^i at $v = 5.84$ is 10.4, and k_G^n at 5.345 is 9.870.

$$k_G \text{ (corrected to } v = 5.84) = 13.02 \times \frac{10.4}{9.87} = 13.72$$

$$\text{lb./hr.ft.}^2 \text{ atm.}$$

3. The evaluation of the constants for equation (24),

p. 44 :

In equation (24)

$$\frac{k_G P_{BM}}{v P_G} = b \left(\frac{v d P}{\mu} \right)^{-m} \left(\frac{\mu}{P D} \right)^{-n}$$

n was selected to be +0.56, and since from the correlation of the data k_G is proportional to the 0.65 power of the relative velocity, m is equal to $1 - 0.65 = 0.35$. The constant b was deduced by inserting the known constants in equation (24). At 20°C, and the common condition of both Fig. 3 and Fig. 4.

$$D_v = 0.892 \text{ ft.}^2/\text{hr. at } 25^\circ\text{C.}$$

$$P = 0.075 \text{ lb./ft.}^3$$

$$P_G = 0.044 \text{ lb./ft.}^3$$

$$\mu = 4.35 \times 10^{-2} \text{ lb./hr.ft.}$$

$$\frac{\mu}{P D} = 0.65 \text{ (dimensionless)}$$

$$P_{BM} = 0.96 \text{ atm.}$$

$$v = 5.84 \text{ ft./sec.} = 21,000 \text{ ft./hr.}$$

$$d = 0.0582 \text{ ft.}$$

$$k_G = 10.4$$

$$k_G = \frac{vP_D}{P_{BH}} \left(\frac{vdp}{\mu} \right)^{-0.35} \left(\frac{\mu}{PD} \right)^{-0.56} b$$

$$= 87b$$

$$b = 0.12$$

The relationship between k_G and \bar{P} has been found to be

$$k_G = 2.96 \bar{P}^{0.26}$$

Since b is a function of the liquid rate, from $k_G = 87b$

$$= 2.96 \bar{P}^{0.26}$$

$$b = 0.034 \bar{P}^{0.26}$$

The final equation is

$$\frac{k_G P_{BH}}{v P_D} = 0.034 \bar{P}^{0.26} \left(\frac{vdp}{\mu} \right)^{-0.35} \left(\frac{\mu}{PD} \right)^{-0.56} \quad (26)$$

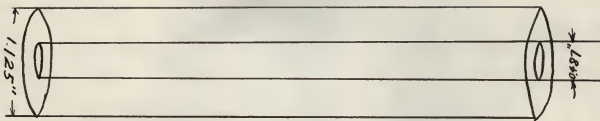
Table 7. List of principal apparatus and material used in this project.

Item	Description	Source
Pyrex column		Corning Glass Co.
Ceramic disc	Unglazed	General Ceramic Co.
Hi-pressure research kit rotameter		Brooks Rotameter Co.
F & P Tri-flat flowrator		Fisher and Porter Co.
Thermal-conductivity cell		Gow-Mac Company
One-half horsepower centrifugal pump	Made of stain- less steel	
CO ₂ gas	Over 99% purity	Pure Carbonic Co.
NH ₃ gas	Anhydrous	Spencer Chemical Co.
N ₂ gas	Water pumped	National Gas Co.

Calculation of Surface Velocity of Falling Film

The following method was used for the calculation of the falling velocity of the liquid layer in the disc column.

The assumption is made that, instead of the series of discs, there is a cylindrical tube erecting in the center of the column with an outside surface area just equal to that of the discs. This equivalent cylinder is shown as follows:



Total surface area of discs

$$= \frac{35}{144} \left[2 \frac{\pi}{4} (0.594)^2 + 0.594 \pi \times 0.188 \right]$$

$$= 0.22 \text{ sq. ft.}$$

Total length of discs

$$= 35 \times 0.594$$

$$= 20.79 \text{ in.}$$

$$= 1.73 \text{ ft.}$$

Diameter of the equivalent cylinder

$$= \frac{0.22}{1.73 \pi} \times 12$$

$$= 0.487''$$

Assume that the thickness of the falling film is the same over the entire length of the cylinder and denoted by X.

$$\begin{aligned} \text{Then the volume of liquid attached to the surfaces of discs} \\ &= X \times \text{total surface area of discs} \\ &= 0.22X \end{aligned}$$

Let Q denote the flow rate of liquid expressed in cu. ft./hr.

Then the surface velocity of the falling film

$$= \frac{1.73}{0.22X} \times Q$$

The film thickness is calculated by Nusselt's equation,

$$\bar{\pi} = \frac{\rho_L^2 g X^3}{3 \mu_L} \quad (20)$$

where X = thickness of the falling liquid film, ft.

g = gravitation const.

ρ_L = liquid density

μ_L = liquid viscosity

$\bar{\pi}$ = liquid flow rate per unit channel perimeter (lb./hr. ft.)

$$\text{or } X = \sqrt[3]{\frac{3 \bar{\pi} \mu_L}{\rho_L^2 g}}$$

Surface velocity

$$= \frac{1.73}{0.22} \times Q \times \sqrt[3]{\frac{\rho_L^2 g}{3 \bar{\pi} \mu_L}}$$

Since $\bar{\pi} = \rho_L \cdot Q/R$

where R = mean perimeter of liquid flow

Mean surface velocity

$$\begin{aligned}
 &= \frac{1.73}{0.22} \times Q \times \sqrt[3]{\frac{\rho^2 g \times 0.127}{3 \rho Q \mu_L}} \quad \text{ft./hr.} \\
 &= \frac{1.73}{0.22 \times 60} \times Q \times \sqrt[3]{\frac{0.127 \rho g}{3 Q \mu_L}} \quad \text{ft./min.} \\
 &= \frac{1.73}{0.22 \times 60} \times \sqrt[3]{\frac{(3600)^2 \times 32.2 \times 0.127}{3}} \sqrt[3]{\frac{Q^2 \rho}{\mu_L}} \quad \text{ft./min.} \\
 &= 34.05 \sqrt[3]{\frac{\rho Q^2}{\mu_L}} \quad \text{ft./min.}
 \end{aligned}$$

In actual operation

Flow rate 60 - 400 lb./hr. ft.

or 0.815 cu. ft./hr.

$\rho_2 = 62.4$ lb./cu. ft.

$\mu_L = 1.85$ lb./hr. ft.

at $\mathcal{P} = 400$ lb./hr. ft. (0.815 cu. ft./hr.)

Mean surface velocity = $34.05 \times \sqrt[3]{\frac{62.4 \times 0.815}{1.85}}$

$$= 34.05 \times \sqrt[3]{\frac{50.86}{1.85}}$$

$$= 34.05 \times 3.02$$

$$= 102.8 \text{ ft./min.}$$

$$= 1.71 \text{ ft./sec.}$$

For turbulent flow $V_{\max.} = \frac{V_{\text{ave}}}{0.8}$

Surface velocity

$$= \frac{1.71}{0.8} = 2.14 \text{ ft./sec.}$$

Principal Constants of the Disc Column

Number of discs	35
Diameter of the disc	1.5 cm. (0.594 inch)
Thickness of the disc	0.48 cm. (0.188 inch)
Diameter of the Pyrex column	1 1/8 inches
Mean perimeter for liquid flow	0.127 ft.
Equivalent diameter for gas flow*	0.059 ft.
Absorption surface*	0.22 sq. ft.

* Dry basis.

Nomenclature

a = effective area, $\text{ft.}^2/\text{ft.}^3$ packed volume

a_d = specific area of dry packing, $\text{ft.}^2/\text{ft.}^3$ packed volume

C_A = concentration of dissolved solute gas, $\text{lb.}/\text{ft.}^3$

C_{A1}, C_1 = concentration of dissolved solute gas, $\text{lb.}/\text{ft.}^3$

C_B = bulk liquid concentration, $\text{lb.}/\text{ft.}^3$

d = equivalent diameter for gas flow, ft.

D = diffusivity, $\text{ft.}^2/\text{hr.}$

D_A = diffusivity of dissolved solute gas, $\text{ft.}^2/\text{hr.}$

D_B = diffusivity of liquid reactant, $\text{ft.}^2/\text{hr.}$

G = mass rate of gas flow, $\text{lb.}/\text{hr.}$

H = Henry's law constant, defined by $p = HC$

k = reaction rate constant

k_I = reaction rate constant for a first-order reaction

k_{II} = reaction rate constant for a second-order reaction

k_G = gas-film transfer coefficient, $\text{lb.}/\text{hr. ft.}^2 \text{ atm.}$

- k_L = liquid-film transfer coefficient, lb./hr. ft.² lb./ft.³
 k_L^i = liquid-film transfer coefficient for physical absorption, lb./hr. ft.² lb./ft.³
 k_s = surface transfer coefficient
 K_G = overall transfer coefficient, lb./hr. ft.² atm.
 L = liquid rate, lb./hr. ft.²
 N_A = rate of mass transfer of solute gas, lb./hr. ft.²
 p = partial pressure of solute in gas, atm.
 p_{BM} = mean partial pressure of inert gas, atm.
 q = concentration of absorbent, lb./ft.³
 s = rate of renewal of liquid surface
 t = temperature of liquid, ° C.
 v = relative velocity of gas to liquid surface, ft./hr.
 x_L = fictitious liquid-film thickness
 X_1 = concentration of solute in effluent, lb./lb.
 X_1^* = concentration of solute in effluent in equilibrium with the partial pressure of the solute gas, lb./lb.
 X_2 = concentration of solute in inlet liquid, lb./lb.
 X_2^* = concentration of solute in inlet in equilibrium with the partial pressure of the solute gas at outlet, lb./lb.
 Y_1 = inlet gas concentration, lb. solute/lb. inert gas
 Y_2 = exit gas concentration, lb. solute/lb. inert gas
 ρ = density, lb./ft.³
 μ = viscosity, lb./hr. ft.
 \mathcal{P} = rate of liquid layer, lb./hr. ft.

GAS ABSORPTION WITH CHEMICAL REACTION

by

CHUNG-KONG HWU

B. S., National Taiwan University, China, 1951

AN ABSTRACT OF A THESIS

submitted in partial fulfillment of the

requirements for the degree

MASTER OF SCIENCE

Department of Chemical Engineering

KANSAS STATE COLLEGE
OF AGRICULTURE AND APPLIED SCIENCE

1954

The purpose of this thesis was to design, construct and calibrate a new type of laboratory column as a versatile research tool for the study of gas absorption with chemical reactions and to perfect the operational and analytical procedures as a guide for subsequent investigations.

The construction has been completed for a "disc column" with 35 ceramic discs having 1.5 cm. diameter and 0.48 cm. thickness. These discs are threaded edgewise and suspended vertically and centrally inside a 1.125" i. d. Pyrex tube. In operation, liquid flows over the surface of the discs in thin layers and gas flows in the space between the discs and the tube wall. The construction includes also such components as necessary for the measurement and control of flow rate, temperature and pressure.

The performance characteristics of this column has been evaluated in two series of experiments. The liquid film mass transfer coefficients were determined from the absorption of carbon dioxide in water; the gas-film coefficients were determined from the absorption of dilute ammonia in water. Empirical equations similar to the general correlation of the wetted wall column coefficients were developed for the purpose of extrapolation to other systems and conditions.

For the liquid-film coefficient,

$$\frac{k_L'}{D} = 3.08 \left(\frac{4\pi}{\mu} \right)^{0.97} \left(\frac{\mu}{PD} \right)^{0.5} \text{ ft.}^{-1}$$

For the gas-film coefficient,

$$\frac{k_G \frac{P}{v}}{P} = 0.034 \pi^{0.26} \left(\frac{v \rho}{\mu} \right)^{0.35} \left(\frac{\mu}{PD} \right)^{-0.56}$$

The exponents of N in both equations are high as compared with other columns. This indicates a pronounced influence of liquid flow rate upon the mass transfer. Also the observed transfer coefficients are numerically lower than those reported elsewhere indicating a comparatively slow specific rate of absorption. These apparent discrepancies are tentatively attributed to the surface characteristics and the dimensions of the discs. Since this column was intended for the study of gas absorption with simultaneous chemical reactions where the variation of the resistance on the liquid side was of primary interest, these unexpected column characteristics may prove to be especially advantageous.